ENVIRONMENTAL RESEARCH
LETTERS

OPEN ACCESS

RECEIVED
22 February 2023

REVISED
18 April 2023

ACCEPTED FOR PUBLICATION
9 May 2023

PUBLISHED
19 May 2023

LETTER

Landscape restoration and greening in Africa

Jessica Ruijsch[1,*], Adriaan J Teuling[2], Jan Verbesselt[3] and Ronald W A Hutjes[1]

1 Water Systems and Global Change Group, Wageningen University and Research, Wageningen, The Netherlands
2 Hydrology and Quantitative Water Management Group, Wageningen University and Research, Wageningen, The Netherlands
3 Laboratory of Geo-information Science and Remote Sensing, Wageningen University and Research, Wageningen, The Netherlands
* Author to whom any correspondence should be addressed.

E-mail: jessica.ruijsch@wur.nl

Keywords: land restoration, regreening, remote sensing, Google Earth Engine, Africa

Supplementary material for this article is available online

Abstract

As a reaction to ongoing environmental change, many local land restoration projects have emerged that aim to prevent or reverse land degradation, combat climate change through carbon sequestration or improve the local climate. However, the contribution of these projects to the greening of Africa at larger scales is still unknown due to the absence of a (public) complete database of land restoration projects, the lack of monitoring and the low survival rate of planted vegetation. Here, we use climate independent greening time series to detect local greening hotspots in Africa. We find that 2.1% of Africa, an area of roughly 400 000 km^2, experiences local greening, especially in semi-arid environments. We show that various forms of sustainable land management (SLM) lead to significant local greening and demonstrate that some forms, e.g. active revegetation, are more effective than others, e.g. natural regeneration. This study, therefore, provides a first continental-scale insight in the greening potential of land restoration, which is needed for a thorough understanding of the effectiveness of SLM.

1. Introduction

Despite the increasing efforts to halt environmental change [1], land degradation continues to affect an estimated 1.3–3.2 billion people worldwide [2, 3], of which the majority lives in developing countries [4]. African drylands such as the Sahel are particularly vulnerable to the effects of land degradation and climate change due water scarcity and population growth [5–7]. Recognizing these pressures we put on key ecosystems, the United Nations declared 2021–2030 to be the Decade of Ecosystem Restoration to support efforts preventing global ecosystem degradation and increase awareness of the importance of restoration [8]. In addition, several organisations have taken the ambitious plan to restore millions of hectares of land in the coming decades by planting billions of trees in African drylands as well as other parts of the world (e.g. the Bonn Challenge, the African Forest Landscape Restoration initiative (AFR100) or the African Great Green Wall initiative [6]). Furthermore, land restoration and tree planting projects have also become a widely recognized approach to combat climate change through carbon sequestration [9–11] or by changing the biophysical properties of the land surface [12–15]. Some researchers even argue that land restoration may be one of the most effective methods for climate change mitigation [16].

As a result, the number of land restoration projects in Africa has rapidly increased over the years [1]. Monitoring these projects is often done with remote sensing products such as the Normalized Difference Vegetation Index (NDVI) [17] or the Enhanced Vegetation Index (EVI), as field measurements are often time-intensive, costly and, in case of remote or large areas, practically impossible. Using these vegetation indices in combination with, for example, a before/after control/impact type of designs [18, 19] has been used to estimate the changes in greenness and vegetation productivity of projects with a known location. However, the lack of a complete and publicly accessible database of land restoration projects in Africa, the considerable number of organizations that work on this [1] and the reported low survival rates of planted vegetation [20–23], make these methods less suitable to evaluate the greening of land restoration projects and their climate change mitigation and adaptation potential on a continental scale.

On top of that, the African continent is not only affected by greening due to small-scale processes such as land restoration, but also by large-scale and long-term greening and browning trends. In the 1970s and 1980s Africa has experienced severe large-scale droughts, which are now attributed to the El Niño-Southern Oscillation and changes in sea surface temperature [24, 25]. Contrarily, observations over the last decades have shown an overall increasing trend in vegetation cover across Africa [14, 26], which is likely caused by an increase in global CO_2 concentration [26] and an increase in precipitation due to changes in sea surface temperature [27–30].

Due to the co-existence of small-scale greening caused by land restoration, and this large-scale 'background' greening, simply monitoring changes in vegetation indices does not tell us the effectiveness of land restoration projects or its contribution to the greening of Africa, but rather shows the combined effect of land management and natural climate variability. To compensate for this effect, previous studies have used vegetation-rainfall relations [31], which can partly account for background trends because it provides an indicator of vegetation or ecosystem functioning. Yet, vegetation-rainfall relationships are complex and often differ over biomes, making it less suitable to study vegetation productivity over large scales [32, 33]. In addition, vegetation-rainfall relations do not consider background trends other than rainfall variability, while literature suggests that CO_2 fertilization causes roughly 70% of the observed greening [26].

Alternatively, we can use spatial-context to separate the small-scale or 'local' greening from large-scale background trends. In this approach, it is assumed that background trends due to natural climate variability act on a much larger scale than a land restoration project [34]. For example, if the greening at a land restoration project is the result of natural climate variability rather than the project itself, surrounding areas will likely show a similar amount of greening as the project area. Contrastingly, if the greening is caused by the project, it is expected that the project area shows a larger amount of greening than surrounding areas. For this reason, the background trends can be removed from vegetation index time series by comparing observed greening trends with surrounding areas.

Here, we apply this spatial-context method to NDVI and EVI time series in Google Earth Engine [35] to (1) create a map of local greening hotspots for Africa, (2) compare the spatial distribution of local greening to background greening, and (3) compare local greening to a publicly available database of sustainable land management (SLM) projects to determine the effectiveness of land restoration. Although spatial-context methods have been used before to detect deforestation [34, 36], land degradation [37, 38] or burned areas [39] in forested as well as grassland areas, this is, to our knowledge, the first time that such a spatial-context method is used to detect local greening hotspots on a continental scale in Africa.

2. Materials and methods

2.1. Input data and study area

We used four different input variables (table 1). The main input data consists of NDVI [40] and EVI [41] time series data (extended data figure 1), which we used as an indicator for vegetation productivity. The main analysis is performed using NDVI and EVI data from the Moderate-Resolution Imaging Spectroradiometer (MODIS) [40] because it is a good compromise between spatial and temporal resolution and the readily availability of quality controlled vegetation index composites. We used Landsat-7 data on a small sample area to explore the effects of a higher spatial resolution on our results (extended data figure 10). Furthermore, we used land cover (45) and aridity index (AI) data to provide some insight into potential causes of local greening. The AI is a measure of dryness and can be defined as a 30-year average fraction between precipitation and potential evapotranspiration [42], which we used to divide the study area into hyper-arid, semi-arid, dry subhumid and humid regions [43]. To evaluate the effect of land restoration practices on the amount of local greening, we used 434 SLM projects from the World Overview of Conservation Approaches and Technologies (WOCAT) database [44] within the study area. This database contains often-used land restoration techniques, such as tree planting or assisted natural regeneration, but also techniques like sustainable agriculture and water harvesting. Here, the whole database of SLM projects is used to study the process of land restoration, meaning we used a broader definition of the term land restoration than other studies (e.g. UNCCD [7] or IUCN [45]). If a single SLM project contained multiple locations, we considered it as multiple projects, resulting in 628 project locations. We categorized these projects into 11 categories and 55 subcategories based on their description, where the categories of 'revegetation' and 'natural regeneration' are highlighted in the results. We refer to the combination of all categories simply as 'sustainable land management' (SLM) (table 2). The study area consists of areas on the African continent with a median NDVI higher than 0.15 or EVI higher than 0.11, which results in similar case study boundaries for the NDVI and EVI. This way, areas with a too low vegetation cover are not considered in the calculations to prevent noisy results. The masked areas mainly consist of the Sahara Desert and constitute 36% of the African continent (extended data figure 1).

Table 1. Overview of input data.

Name	Source	Spatial resolution	Temporal resolution	Time period	Reference
NDVI	Terra MODIS Vegetation Indices (MOD13Q1.006)	250 m	16-day composites	2001-01-01 to 2022-01-01	[40]
	USGS Landsat-7 ETM+ Level2, Collection 2, Tier 1	30 m	16-day land surface reflectance images	2001-01-01 to 2022-01-01	USGS
EVI	Terra MODIS Vegetation Indices (MOD13Q1.006)	250 m	16-day composites	2001-01-01 to 2022-01-01	[40]
Land cover	MODIS Land Cover Type (MCD12Q1)	1 km	Yearly	2001	[46]
Aridity index	CRU TS4.04	0.5°	Yearly	1991 to 2029	[47, 48]
SLM projects	WOCAT SLM technologies	Point coordinates	—	—	[44]

Table 2. Description of categories of WOCAT sustainable land management projects highlighted in this study. An overview of all categories is given in extended data figure 10.

Category	Description	Project categories included
Sustainable land management	'The use of land resources, including soils, water, animals and plants, for the production of goods to meet changing human needs, while simultaneously ensuring the long-term productive potential of these resources and the maintenance of their environmental functions' [44]. WOCAT mainly focusses on preventing and reducing land degradation	All WOCAT SLM projects, e.g. runoff harvesting, alternative cooking methods, riverbank restoration, planting trees, area closure, fire management, cover crops, agroforestry and conservation agriculture.
Revegetation	Active planting of vegetation species to accelerate vegetation regrowth.	Planting (fruit) trees, shrubs and grasses, implementing vegetation strips, and projects described as restoration.
Natural regeneration	A passive method of regreening, where vegetation cover is increased through natural regrowth by using, for example, area closure, grazing management or management of invasive species.	Assisted natural regeneration, combating invaders, farmer managed natural regeneration, area closure, grazing management and bush thinning.

2.2. Spatial-context approach

To separate background trends from the NDVI and EVI time series, we used a spatial-context approach. For each pixel, we determined the vegetation index time series over the 2001–2021 period, after which we calculated neighbourhood averaged time series over a square-shaped neighbourhood around the pixel. A square centre with a radius of 1 km, corresponding to a square of 2 × 2 km, was not included in the mean to reduce the influence of the original time series on the mean neighbourhood time series. Next, we subtracted the neighbourhood time series form the centre pixel time series to create 'spatially corrected' time series. Creating this spatially corrected time series for the NDVI and EVI allows us to evaluate the changes in greenness compared to surrounding areas, thus separating greening trends resulting from small-scale processes and land management from those caused by natural climate variability.

In this study, we applied the spatial-context method to three neighbourhood radiuses of 25 km, 10 km and 5 km, corresponding to squares of 50 × 50 km, 20 × 20 km and 10 × 10 km, respectively. We highlight the results of the 25 km radius, which captures the effect of large land restoration efforts without crossing multiple AI classes. The results for 10 km and 5 km radiuses are included in the supplementary data.

2.3. Definition of local greening

We applied the Breaks For Additive Seasonal and Trend (BFAST) algorithm [49–51] for Google Earth Engine [52] to the spatially corrected NDVI and EVI time series. BFAST decomposes the time series into a trend, seasonal and remainder component, by fitting a linear/harmonic model to the time series. Unlike other decomposition algorithms, BFAST can detect significant changes, called breakpoints, in the components, resulting in a piecewise linear harmonic model. We applied BFAST using a seasonal harmonic model order of 3, a minimum spacing between two breakpoints of 0.15 (fraction of total time series length, i.e. 3 year) and a maximum of one breakpoint. Here, we use BFAST instead of linear regression because we expect land restoration to show a sudden change in greenness compared to surrounding areas rather than a gradual change, which BFAST can capture in the form of a breakpoint. We therefore expect the breakpoint to represent the moment a project, or another process, will start to affect vegetation cover.

We defined local NDVI/EVI greening as pixels where: (1) the BFAST algorithm detects a breakpoint in the trend of the spatially corrected NDVI/EVI time series, (2) the computed BFAST trend after the breakpoint is positive, significantly different from zero ($p = 0.05$) and larger than before the breakpoint, and (3) the original (centre pixel) NDVI/EVI time series shows a positive linear trend after the breakpoint (figure 1(A)). We included this last condition, as pixels could theoretically show a greening trend compared to its surroundings, even though the pixel itself is browning. Next, we defined local greening hotspots in Africa as areas that simultaneously experience local NDVI greening and local EVI greening. By combining the NDVI and EVI, we aim to reduce noise and therefore improve the accuracy of this spatial context method.

2.4. Calculation of background trends

To calculate the background trends, we applied linear least squares regression to the original NDVI and EVI data between 2001 and 2021 within the study area (figure 1(B)). We then assigned background greening to pixels that show a significant positive trend for both the NDVI and EVI ($p = 0.05$). Similarly, browning trends show a significant negative trend. Areas that have a positive NDVI trend and a negative EVI trend or vice versa, and areas without a significant trend are considered not to have a background trend.

2.5. Local greening of SLM

Next, we used the WOCAT project database to evaluate the regreening effects of SLM projects. Therefore, we used local greening instead of the often-used background greening, to reduce the effects of large-scale processes such as natural climate variability, which makes it more likely that observed greening is due to the changes in land management. Because WOCAT only contains point coordinates of projects instead of boundaries, we cannot directly calculate the amount of local greening inside the project. Instead, we computed the percentage of local greening pixels in a circle around the project's geo-tag multiple times, using a radius of 5000, 4000, 3000, 2000, 1000 and 500 m. Next, we computed for each project the percentage of greening pixels over the locations in the study area within the same country, AI class and land cover class as the project (extended data figure 2). We then determined whether SLM projects cause a significant increase in local greening using the two-sided t-test for independent samples, assuming unequal variances and a significance level of 5%.

3. Results

3.1. Spatial distribution of local greening in Africa

Applying the spatial-context method (figure 1(A)) to the African continent with a neighbourhood radius of 25 km, 2.1% of the study area (roughly 400 000 km^2) shows local greening over the last two decades (figure 1(C)). Most of these areas have a breakpoint towards the end of the study period, with peaks around 2015 and 2018, suggesting that many areas start to show an increase in greenness compared to its surroundings around these years (figure 1(E)), although it should be noted that the used settings of the BFAST algorithm do not allow for the detection of breakpoints after 2018. We can also observe that the local greening is not evenly distributed across the continent, as a large part of the local greening can be found in the Sahel, Kenya, Tanzania, and regions in southern Africa (extended data figure 2). Similar spatial distributions can be found for a neighbourhood radius of 10 km and 5 km, although the total area classified as local greening as well as the number of adjacent local greening pixels is smaller (extended data figure 8). For a 10 km and 5 km radius, respectively 1.9% and 1.8% of the study area shows local greening, compared to 2.1% for a 25 km radius.

We also compared the local greening hotspots to NDVI and EVI background trends (figure 1(B)) to provide more insight into the contributions of local greening to the greening of the African continent. Overall, a larger area shows background greening (32.4% of the study area) than local greening (2.1% of the study area), especially in more humid areas such as the Congo Basin in central Africa (figure 1(D); extended data figure 7). These areas do usually not show a breakpoint when BFAST is applied to the spatially corrected NDVI time series, suggesting that a large part of the background trends, especially in humid areas, is not caused by small scale or abrupt processes, but by longer large-scale processes. In other, dryer areas such as in Botswana and Namibia, we observe strong background greening combined with a large amount of local greening pixels, suggesting a combination of large-scale and small-scale processes. Although most local greening in the study area is located in areas that also show a background greening trend (45.1%) or no background trend (41.6%), also a considerable amount of local greening is present in areas that show a long-term browning trend (13.3%) (figure 1(F)). The combination of local greening and background browning suggests a long term linear browning trend, with a sudden increase in greenness, compared to surrounding areas, at the end of the time-series. A similar spatial-context method can of course be used to detect local browning, which occurs at 1.9% of the study area (extended data figure 9).

3.2. Drivers and properties of local greening hotspots

We compared local greening to an aridity and land cover classification and find that 39.1% of the local greening can be found in semi-arid regions, while these regions only cover 26% of the study area (figure 2(H); extended data table 1). Here, 3.0% of the area is found to be greening compared to its neighbourhood. Humid areas, on the other hand, account

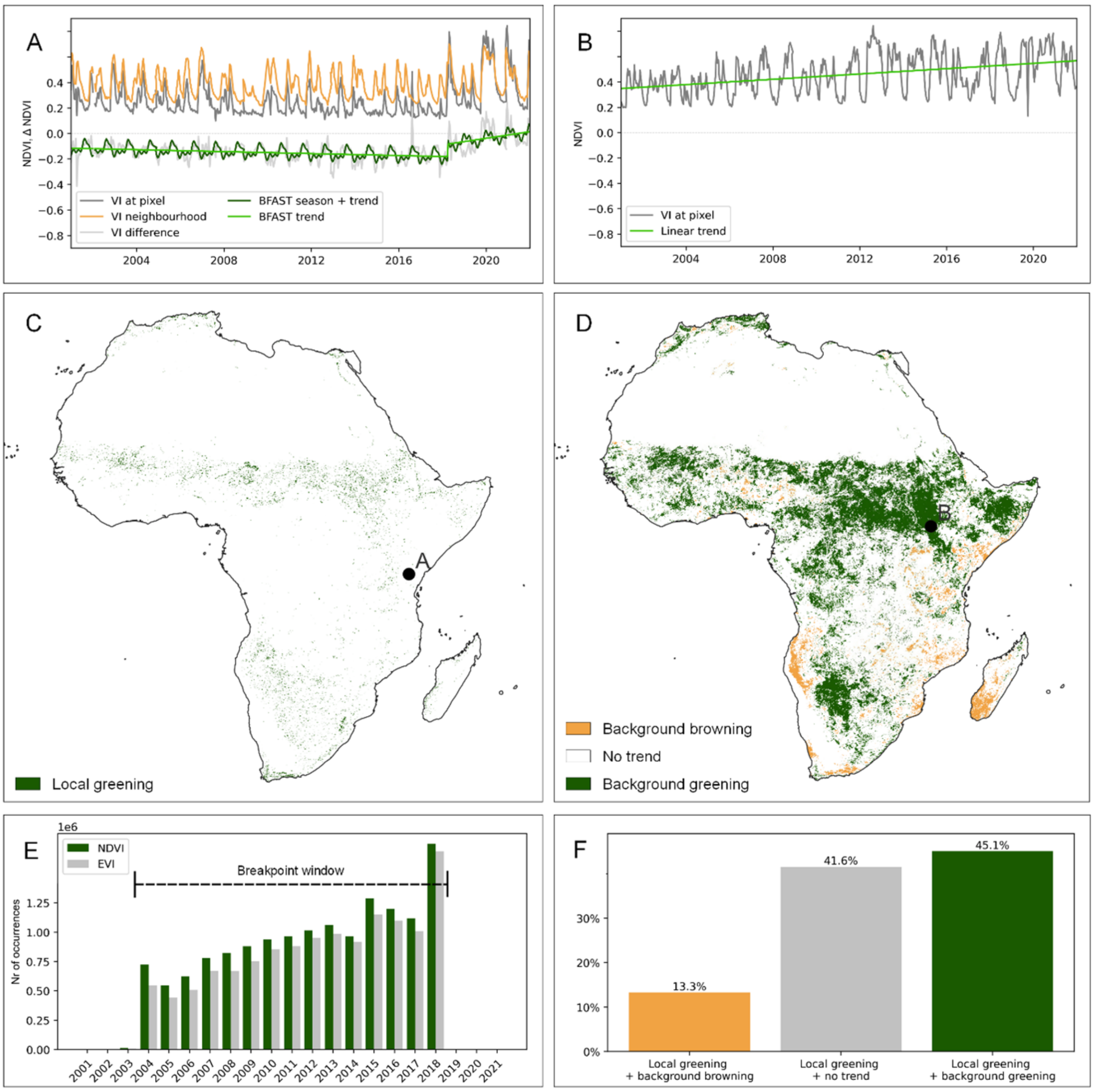

Figure 1. Spatial distribution of local greening and background trends. (A) Illustration of the spatial-context method and (B) the background trends with NDVI time series (a more detailed description of these methods can be found in the methodology section and extended data figure 3). (C) Spatial distribution of the combined NDVI and EVI local greening pixels. Point A shows the location of the time series in figure (A). A larger map of the spatial distribution of local greening of NDVI, EVI and combined pixels is included in extended data figures 4–6. (D) Spatial distribution of the combined NDVI and EVI background trends, calculated with a linear least squares regression. Negative trends are shown as browning, positive trends as greening and non-significant trends as no trend ($p = 0.05$). Point B shows the location of the time series in figure (B). A larger map of the spatial distribution of EVI and NDVI background greening is included in extended data figure 7. (E) Histogram of breakpoint year of the EVI and NDVI local greening pixels. The breakpoint window indicates the years where a breakpoint can be detected by the BFAST algorithm. (F) Distribution of background trends at the location of the combined local greening pixels.

for only 32.0% of the local greening, while covering more than half of the study area. This pattern is also visible in the distribution of the local greening over the land cover types, as most local greening occurs in shrublands, grasslands and savannas, but also areas classified as cropland sometimes show local greening (figure 2(H); extended data table 1).

By visually interpreting high resolution satellite imagery, we also aim to provide some more insight into potential drivers of local greening. Land restoration practices such as in Kenya, show greening between 2014 (figure 2(A) and 2019 (figure 2(B)), while surrounding areas are untreated. Similar results can be found in South-Africa, where local greening pixels are located roughly inside protected areas [53] (figure 2(F)). However, also reduction in open-water surface area, such as in Lake Chad, can cause unwanted classification of local greening (figures 2(C) and (D)). This is caused by the low NDVI value of water and, consequently, a local increase in NDVI when the water retreats. In addition, we observed a reasonably large amount of local greening in agricultural areas such as in the north of Nigeria (figure 3(C)), which is also visible in the histogram (figure 3(H)) and may result from intentional greening efforts.

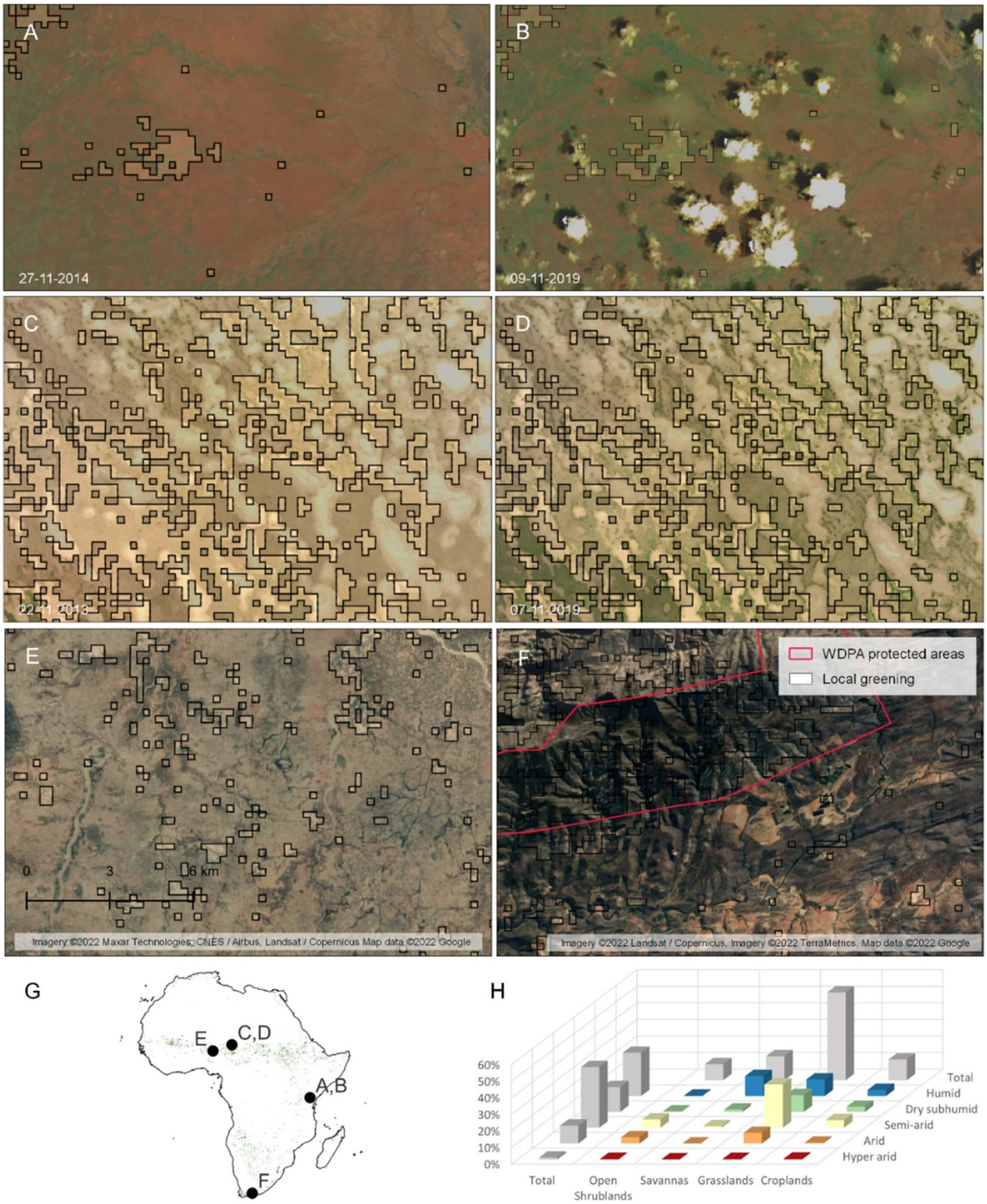

Figure 2. Examples and surface properties of local greening pixels. (A) and (B) Local greening pixels in Kenya where land restoration is implemented. The background contains Landsat 8 imagery [54] from November 2014 (A) and November 2019 (B), which visually shows greening over time. For visualization purposes, the local greening pixels are made lighter compared to the background. (C) and (D) Local greening pixels in Chad along the borders of Lake Chad, showing greening due to changes in water level between 2013 (C) and 2019 (D). (E) Agriculture along riverbanks in Nigeria. (F) Local greening pixels in South-Africa, located in WDPA protected areas [53]. (G) Locations of above examples. The background shows the local greening pixels. (H) Percentage of greening pixels per land use class, aridity class and the combined land use and aridity classes (extended data figure 2). For readability, we did not include the land use and aridity classes that contained less than 5% of the greening pixels. The complete histogram is attached in extended data table 1.

3.3. SLM as driver of local greening

As most of the local greening can be found in semi-arid environments, most SLM projects in these regions also show generally a high percentage of local greening (figure 3(A)). Furthermore, even though projects in more hyper-arid or humid regions show less local greening, SLM projects show an overall significant increase in local greening compared to the areas with similar aridity and land cover for all distances around the project we included in this study (figure 3(B)). Revegetation projects, including the planting of (fruit) trees, shrubs and grasses, have a significant higher percentage of local greening in an area of 500 and 1000 m around the project's geo-tag, while the other radiuses show an increased, yet not significant, local greening. Especially planting trees and fruit

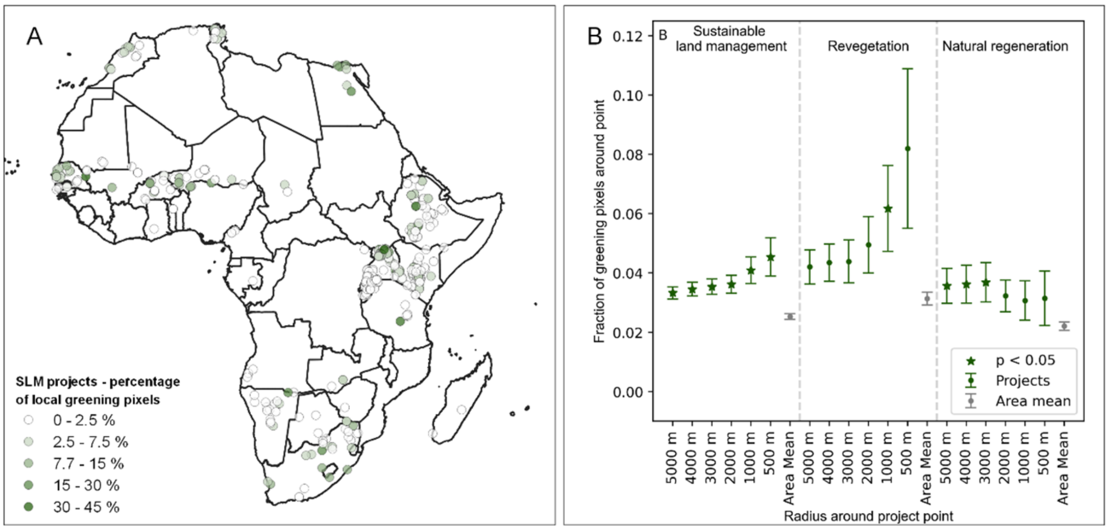

Figure 3. Evaluation of local greening due to sustainable land management (SLM). (A) Location of WOCAT sustainable land management projects. The shade of the colour indicates the percentage of greening pixels inside an area of 2000 m around the point and (B) mean and standard error of the percentage of local greening pixels in areas with different sizes around all sustainable land management projects, revegetation projects and natural regeneration projects. Significant differences with areas with the same land use type, aridity class and countries are marked with a star ($p = 0.05$). The sustainable land management column consists of all projects in the database. The revegetation and natural regeneration columns contain a subset. Projects in Cape Verde and areas with a median NDVI lower than 0.15 are not shown, because they fall outside the study area. Local greening effects of the other subcategories of sustainable land management are visualized in extended data figure 11.

trees seems to have a large effect (extended data figure 11). Natural regeneration projects, such as farmer managed natural regeneration, assisted natural regeneration or area closure, appears to have a lower effect on the amount of local greening than revegetation projects for all area sizes around the project. Yet, there is a significant increase in local greening around 5000, 4000 and 3000 m around the project. Other categories of SLM, such as water harvesting, erosion prevention or agriculture management have a more mixed effect on local greening (extended data figure 11).

4. Discussion and conclusions

In this study, we used a spatial-context approach in Google Earth Engine, to separate small scale greening caused by land restoration and SLM, from background trends due to natural climate variability. With this method, we showed that that 2.1% of the African continent experienced local greening over the 2001–2021 period, especially in semi-arid environments. In more humid regions, we saw less local greening, even though these regions showed significant background greening. This matches with our expectations from the spatial-context method, because changes in land management may result in a larger vegetation cover increase in sparsely vegetated semi-arid regions than in regions that are already densely vegetated. In humid areas it is less likely that small scale processes result in such a large increase in vegetation cover that it would be detected as a breakpoint in the NDVI and EVI time series.

In addition, our results also suggests that even though SLM as a whole has a positive effect on the amount of local greening, revegetation and tree planting appears to be more effective than natural regeneration over smaller areas. Natural regeneration does, however, show a significant increase in local greening pixels around a larger area than active revegetation. This coincides with other studies, that found a faster recovery of highly degraded land due to active restoration practices such as tree planting compared to more passive methods [55, 56]. On the other hand, natural regeneration is, although slower, often much cheaper [57] and can therefore result in the restoration of much larger areas, with a more natural species composition [58] if enough time is available. Therefore, natural regeneration projects may prove to be more effective once a longer study period is available. In addition, we want to emphasize that greening is often not the only goal of SLM and land restoration projects [1], as people also implement land restoration for biodiversity conservation, income generation, legislations or cultural reasons [59]. A lack of local greening found for some projects in this study does therefore not necessarily mean that the SLM project is not at all effective or failed, as greening may not have been the main goal of the project.

Yet, several uncertainties that should be kept in mind when interpreting the spatial-context approach. As we defined local greening as a sudden increase in greenness compared to surrounding areas, it does not only show changes in land restoration, but every type of small-scale greening, including changes in water level or agriculture. This calls for further development of the spatial-context method such that these different causes can be split, allowing for the evaluation of land restoration only. In addition, we evaluated the SLM projects based on a circle around a point coordinate. An exact size and boundary of each project would result in a more accurate evaluation. Furthermore, the moderate spatial resolution (250 m) of MODIS limits the detection of small SLM projects and spatial heterogeneity within these projects. Because 7% of the projects within the WOCAT database reported a size smaller than the spatial resolution of MODIS, there lies great potential in high-resolution satellite imagery or microwave and LiDAR observations, which can detect vegetation optical depth, forest structure or even individual trees and shrubs outside forested areas [60–62]. Unfortunately, higher-resolution imagery usually comes with a lower temporal resolution or shorter data range, which limited their use in this study. In addition, applying the spatial-context method to higher-resolution Landsat-7 data showed similar patterns, but smaller areas of local greening, probably caused by the lower temporal resolution of Landsat-7. This suggests that this data will not result in a more sensitive detection of local greening. Similarly, the spatial-context method is unable to detect greening over areas larger than the used neighbourhood (approximately 2500 km^2), due to uniform greening of the neighbourhood. Fortunately, only 4% of the SLM projects reported to have a size larger than 2500 km^2, although it should be noted that 38% of the projects did not report any project size and oftentimes it is not clear whether this is the actual size of the project or of the region in which it is implemented. Finally, studying seasonal changes of greenness due to land restoration more in depth may provide useful information for policy makers when implementing land restoration projects.

These days, tree planting and land restoration projects are seen as an effective method for climate change mitigation, and are therefore widely included in climate change policy proposals, resulting in ambitions tree planting projects across the world [16, 63]. However, if not implemented correctly, land restoration can also have severe negative consequences on the environment [64], such as a decrease in biodiversity through monocultures or non-native vegetation [65, 66], changes in water availability through increased evapotranspiration [67–69], or the destruction of native ecosystems through displacement of land use [70]. The increasing interests in land restoration thus asks for more research on the cost and benefits of land restoration [71, 72]. However, due the co-existence of small-scale greening and background trends, in combination with the lack of an available (complete) dataset of land restoration projects, it is not known to what extend land restoration actually causes greening. In this study, we provided insight into the hotspots of local greening, as well as an objective meta-evaluation of different types of SLM. We show that implementing SLM projects in semi-arid areas can indeed result in local greening. If the goal of projects is to increase vegetation cover, active revegetation may provide good results on smaller scales, while natural regeneration has the potential to regreen larger areas. Policymakers should therefore carefully match the project approach to its goals, keeping all positive as well as negative consequences of vegetation changes in mind. Yet, even though this research provided a useful monitoring and evaluation tool for land restoration projects, we want to stress the importance of documenting and monitoring the projects its implementation, which would improve the accuracy of the evaluation. We therefore argue that more research should focus on the creation of a complete and open-access database of land restoration projects, before large-scale implementation does more harm than good.

Data availability statements

The data that support the findings of this study are openly available.

View the Google Earth Engine scripts: https://code.earthengine.google.com/2ca1cef5d2c1c81de776624aa8388b86.

Explore data in the Google Earth Engine application: https://jessicaruijsch-wur.users.earthengine.app/view/landscape-restoration-and-greening-in-africa.

The data that support the findings of this study are openly available at the following URL/DOI: https://doi.org/10.6084/m9.figshare.21155335.

Acknowledgments

We gratefully acknowledge the Africa Water Foundation for funding this research. We also thank the reviewers for providing useful comments for improving the initial manuscript.

Author contributions

J R, J R, A J T, J V and R W A H designed research; J R performed research; J R and J V contributed new reagents/analytic tools; J R, A J T, J V and R W A H analysed data; J R, A J T, J V and R W A H wrote the paper.

ORCID iDs

Jessica Ruijsch https://orcid.org/0000-0001-6510-7499
Adriaan J Teuling https://orcid.org/0000-0003-4302-2835
Jan Verbesselt https://orcid.org/0000-0001-7923-4309
Ronald W A Hutjes https://orcid.org/0000-0002-7197-0528

References

[1] Martin M P, Woodbury D J, Doroski D A, Nagele E, Storace M, Cook-Patton S C, Pasternack R and Ashton M S 2021 People plant trees for utility more often than for biodiversity or carbon *Biol. Conserv.* **261** 109224

[2] Gibbs H and Salmon J M 2015 Mapping the world's degraded lands *Appl. Geogr.* **57** 12–21

[3] Le Q B, Nkonya E and Mirzabaev A 2016 Biomass productivity-based mapping of global land degradation hotspots *Economics of Land Degradation and Improvement–A Global Assessment for Sustainable Development* ed E Nkonya, A Mirzabaev and J von Braun (New York: Springer) pp 55–84

[4] Barbier E B and Hochard J P 2018 Land degradation and poverty *Nat. Sustain.* **1** 623–31

[5] Closset M, Feindouno S, Guillaumont P and Simonet C 2017 A physical vulnerability to climate change index: which are the most vulnerable developing countries? (https://doi.org/hal-01719925v3)

[6] UNCCD 2020 *The Great Green Wall Implementation Status and Way Ahead to 2030*

[7] UNCCD 2017 *Global Land Outlook* 1st edn (Bonn: Secretariat of the United Nations Covention to Combat Desertification)

[8] UNEP 2019 Resolution 73/284: United Nations Decade on Ecosystem Restoration (2021–2030)

[9] IPCC 2019 Climate change and land *An IPCC special report on climate change, desertification, land degradation, sustainable land management, food security, and greenhouse gas fluxes in terrestrial ecosystems* (IPCC)

[10] Shevliakova E, Stouffer R J, Malyshev S, Krasting J P, Hurtt G C and Pacala S W 2013 Historical warming reduced due to enhanced land carbon uptake *Proc. Natl Acad. Sci.* **110** 16730–5

[11] Friedlingstein P *et al* 2020 Global carbon budget 2020 *Earth Syst. Sci. Data* **12** 3269–340

[12] Mahmood R, Pielke Sr R A, Hubbard K G, Niyogi D, Dirmeyer P A and McAlpine C *et al* 2014 Land cover changes and their biogeophysical effects on climate *Int. J. Climatol.* **34** 929–53

[13] Perugini L, Caporaso L, Marconi S, Cescatti A, Quesada B, de Noblet-ducoudre N, House J I and Arneth A 2017 Biophysical effects on temperature and precipitation due to land cover change *Environ. Res. Lett.* **12** 053002

[14] Piao S *et al* 2020 Characteristics, drivers and feedbacks of global greening *Nat. Rev. Earth Environ.* **1** 14–27

[15] Spracklen D, Baker J, Garcia-Carreras L and Marsham J 2018 The effects of tropical vegetation on rainfall *Annu. Rev. Environ. Resour.* **43** 193–218

[16] Bastin J-F, Finegold Y, Garcia C, Mollicone D, Rezende M, Routh D, Zohner C M and Crowther T W 2019 The global tree restoration potential *Science* **365** 76–79

[17] Tucker C J 1979 Red and photographic infrared linear combinations for monitoring vegetation *Remote Sens. Environ.* **8** 127–50

[18] Underwood A 1992 Beyond BACI: the detection of environmental impacts on populations in the real, but variable, world *J. Exp. Mar. Biol. Ecol.* **161** 145–78

[19] Meroni M, Schucknecht A, Fasbender D, Rembold F, Fava F, Mauclaire M, Goffner D, di Lucchio L M and Leonardi U 2017 Remote sensing monitoring of land restoration interventions in semi-arid environments with a before–after control-impact statistical design *Int. J. Appl. Earth Obs. Geoinf.* **59** 42–52

[20] Nunes A *et al* 2016 Ecological restoration across the Mediterranean Basin as viewed by practitioners *Sci. Total Environ.* **566** 722–32

[21] Kodikara K A S, Mukherjee N, Jayatissa L P, Dahdouh-Guebas F and Koedam N 2017 Have mangrove restoration projects worked? An in-depth study in Sri Lanka *Restor. Ecol.* **25** 705–16

[22] Murekezi J, Nduwamungu J and Munyanziza E 2013 Investigation of survival rate of trees planted in agroforestry and forest plantations in HuyeDistrict from 2007 to 2011 and underlying factors *Rwanda J.* **1** 52–61

[23] Trac C J, Harrell S, Hinckley T M and Henck A C 2007 Reforestation programs in Southwest China: reported success, observed failure, and the reasons why *J. Mt. Sci.* **4** 275–92

[24] Giannini A, Biasutti M and Verstraete M M 2008 A climate model-based review of drought in the Sahel: desertification, the re-greening and climate change *Glob. Planet. Change* **64** 119–28

[25] Masih I, Maskey S, Mussá F and Trambauer P 2014 A review of droughts on the African continent: a geospatial and long-term perspective *Hydrol. Earth Syst. Sci.* **18** 3635–49

[26] Zhu Z *et al* 2016 Greening of the Earth and its drivers *Nat. Clim. Change* **6** 791–5

[27] Giannini A 2015 Hydrology: climate change comes to the Sahel *Nat. Clim. Change* **5** 720–1

[28] Giannini A, Saravanan R and Chang P 2003 Oceanic forcing of Sahel rainfall on interannual to interdecadal time scales *Science* **302** 1027–30

[29] Biasutti M 2019 Rainfall trends in the African Sahel: characteristics, processes, and causes *Wiley Interdiscip. Rev. Clim. Change* **10** e591

[30] Ouedraogo I, Runge J, Eisenberg J, Barron J and Sawadogo-Kaboré S 2014 The re-greening of the Sahel: natural cyclicity or human-induced change? *Land* **3** 1075–90

[31] Houérou HN L 1984 Rain use efficiency: a unifying concept in arid-land ecology *J. Arid Environ.* **7** 213–47

[32] Horion S, Cornet Y, Erpicum M and Tychon B 2013 Studying interactions between climate variability and vegetation dynamic using a phenology based approach *Int. J. Appl. Earth Obs. Geoinf.* **20** 20–32

[33] Huxman T E *et al* 2004 Convergence across biomes to a common rain-use efficiency *Nature* **429** 651–4

[34] Hamunyela E, Verbesselt J and Herold M 2016 Using spatial context to improve early detection of deforestation from Landsat time series *Remote Sens. Environ.* **172** 126–38

[35] Gorelick N, Hancher M, Dixon M, Ilyushchenko S, Thau D and Moore R 2017 Google Earth Engine: planetary-scale geospatial analysis for everyone *Remote Sens. Environ.* **202** 18–27

[36] Lhermitte S, Verbesselt J, Verstraeten W W and Coppin P 2011 A comparison of time series similarity measures for classification and change detection of ecosystem dynamics *Remote Sens. Environ.* **115** 3129–52

[37] Abel C, Horion S, Tagesson T, Brandt M and Fensholt R 2019 Towards improved remote sensing based monitoring of dryland ecosystem functioning using sequential linear regression slopes (SeRGS) *Remote Sens. Environ.* **224** 317–32

[38] Abel C *et al* 2020 The human–environment nexus and vegetation–rainfall sensitivity in tropical drylands *Nat. Sustain.* **4** 1–8

[39] Lhermitte S, Verbesselt J, Verstraeten W W and Coppin P 2010 A pixel based regeneration index using time series similarity and spatial context *Photogramm. Eng. Remote Sens.* **76** 673–82

[40] Didan K 2015 MOD13Q1 MODIS/Terra Vegetation Indices 16-Day L3 Global 250m SIN Grid V006 *NASA EOSDIS Land Processes DAAC* (https://doi.org/10.5067/MODIS/MOD13Q1.006)

[41] Huete A R, Liu H and van Leeuwen W J (eds) 1997 The use of vegetation indices in forested regions: issues of linearity and saturation *IGARSS'97 1997 IEEE Int. Geoscience and Remote Sensing Symp. Proc. Remote Sensing-A Scientific Vision for Sustainable Development* (IEEE) (https://doi.org/10.1109/IGARSS.1997.609169)

[42] Cherlet M, Hutchinson C, Reynolds J, Hill J, Sommer S and von Maltitz G E 2018 *World Atlas of Desertification* 3rd edn (Luxembourg: Publication Office of the European Union)

[43] Middleton N and Thomas D 1997 *World Atlas of Desertification* 2nd edn (New York: Wiley)

[44] WOCAT Global sustainable land management database *Technologies WOoCAa* (available at: www.wocat.net/en/2022)

[45] IUCN 2019 Reviving land and restoring landscapes *Policy Convergence Between Forest Landscape Restoration And Land Degradation Neutrality* (Gland: IUCN)

[46] Sulla-Menashe D, Gray J M, Abercrombie S P and Friedl M A 2019 Hierarchical mapping of annual global land cover 2001 to present: The MODIS Collection 6 Land Cover product *Remote Sens. Environ.* **222** 183–94

[47] Harris I C, Jones P D and Osborn T CRU TS4.04: Climatic Research Unit (CRU) Time-Series (TS) version 4.04 of high-resolution gridded data of month-by-month variation in climate (January 1901-December 2019) *Analysis UoEACRUCfED* (available at: https://catalogue.ceda.ac.uk/uuid/89e1e34ec3554dc98594a5732622bce92020)

[48] Spinoni J, Vogt J, Naumann G, Carrao H and Barbosa P 2015 Towards identifying areas at climatological risk of desertification using the Köppen–Geiger classification and FAO aridity index *Int. J. Climatol.* **35** 2210–22

[49] Verbesselt J, Hyndman R, Newnham G and Culvenor D 2010 Detecting trend and seasonal changes in satellite image time series *Remote Sens. Environ.* **114** 106–15

[50] Verbesselt J, Hyndman R, Zeileis A and Culvenor D 2010 Phenological change detection while accounting for abrupt and gradual trends in satellite image time series *Remote Sens. Environ.* **114** 2970–80

[51] Verbesselt J, Zeileis A and Herold M 2012 Near real-time disturbance detection using satellite image time series *Remote Sens. Environ.* **123** 98–108

[52] Hamunyela E, Rosca S, Mirt A, Engle E, Herold M, Gieseke F and Verbesselt J 2020 Implementation of BFASTmonitor algorithm on Google Earth Engine to support large-area and sub-annual change monitoring using earth observation data *Remote Sens.* **12** 2953

[53] UNEP-WCMC Protected Area Profile for South Africa from the World Database on Protected Areas (available at: www.protectedplanet.net2022)

[54] Irons J R, Dwyer J L and Barsi J A 2012 The next Landsat satellite: the Landsat data continuity mission *Remote Sens. Environ.* **122** 11–21

[55] Zahawi R A, Reid J L and Holl K D 2014 Hidden costs of passive restoration *Restor. Ecol.* **22** 284–7

[56] Toledo-Aceves T, Trujillo-Miranda A L and López-Barrera F 2021 Tree regeneration in active and passive cloud forest restoration: functional groups and timber species *For. Ecol. Manage.* **489** 119050

[57] Prach K and del Moral R 2015 Passive restoration is often quite effective: response to Zahawi *et al* (2014) *Restor. Ecol.* **23** 344–6

[58] Bechara F C, Dickens S J, Farrer E C, Larios L, Spotswood E N, Mariotte P and Suding K N 2016 Neotropical rainforest restoration: comparing passive, plantation and nucleation approaches *Biodivers. Conserv.* **25** 2021–34

[59] Brancalion P H and Holl K D 2020 Guidance for successful tree planting initiatives *J. Appl. Ecol.* **57** 2349–61

[60] Brandt M, Rasmussen K, Peñuelas J, Tian F, Schurgers G, Verger A, Mertz O, Palmer J R B and Fensholt R 2017 Human population growth offsets climate-driven increase in woody vegetation in sub-Saharan Africa *Nat. Ecol. Evol.* **1** 1–6

[61] Tang H, Armston J, Hancock S, Marselis S, Goetz S and Dubayah R 2019 Characterizing global forest canopy cover distribution using spaceborne lidar *Remote Sens. Environ.* **231** 111262

[62] Brandt M *et al* 2020 An unexpectedly large count of trees in the West African Sahara and Sahel *Nature* **587** 78–82

[63] Fagan M E, Reid J L, Holland M B, Drew J G and Zahawi R A 2020 How feasible are global forest restoration commitments? *Conserv. Lett.* **13** e12700

[64] Holl K D and Brancalion P H 2020 Tree planting is not a simple solution *Science* **368** 580–1

[65] Veldman J W *et al* 2019 Comment on 'The global tree restoration potential' *Science* **366** eaay7976

[66] Veldman J W, Overbeck G E, Negreiros D, Mahy G, Le Stradic S, Fernandes G W, Durigan G, Buisson E, Putz F E and Bond W J 2015 Where tree planting and forest expansion are bad for biodiversity and ecosystem services *BioScience* **65** 1011–8

[67] Feng X *et al* 2016 Revegetation in China's Loess Plateau is approaching sustainable water resource limits *Nat. Clim. Change* **6** 1019–22

[68] Filoso S, Bezerra M O, Weiss K C and Palmer M A 2017 Impacts of forest restoration on water yield: a systematic review *PLoS One* **12** e0183210

[69] van Dijke Aj H, Herold M, Mallick K, Benedict I, Machwitz M, Schlerf M, Pranindita A, Theeuwen J J E, Bastin J-F and Teuling A J 2022 Shifts in regional water availability due to global tree restoration *Nat. Geosci.* **15** 363–8

[70] Meyfroidt P, Rudel T K and Lambin E F 2010 Forest transitions, trade, and the global displacement of land use *Proc. Natl Acad. Sci.* **107** 20917–22

[71] Cooke S J, Bennett J R and Jones H P 2019 We have a long way to go if we want to realize the promise of the 'Decade on Ecosystem Restoration' *Conserv. Sci. Pract.* **1** e129

[72] Dudley N, Eufemia L, Fleckenstein M, Periago M E, Petersen I and Timmers J F 2020 Grasslands and savannahs in the UN Decade on Ecosystem Restoration *Restor. Ecol.* **28** 1313–7